Neuronal somatic ATP release triggers neuron–satellite glial cell communication in dorsal root ganglia

X. Zhang, Y. Chen, C. Wang, and L.-Y. M. Huang*

Department of Neuroscience and Cell Biology, University of Texas Medical Branch, Galveston, TX 77555-1069

Edited by Charles F. Stevens, The Salk Institute for Biological Studies, La Jolla, CA, and approved April 25, 2007 (received for review December 14, 2006)

It has been generally assumed that the cell body (soma) of a neuron, which contains the nucleus, is mainly responsible for synthesis of macromolecules and has a limited role in cell-to-cell communication. Using sniffer patch recordings, we show here that electrical stimulation of dorsal root ganglion (DRG) neurons elicits robust vesicular ATP release from their somata. The rate of release events increases with the frequency of nerve stimulation; external Ca^{2+} entry is required for the release. FM1–43 photoconversion analysis further reveals that small clear vesicles participate in exocytosis. In addition, the released ATP activates P2X7 receptors in satellite cells that enwrap each DRG neuron and triggers the communication between neuronal somata and glial cells. Blocking L-type Ca^{2+} channels completely eliminates the neuron–glia communication. We further show that activation of P2X7 receptors can lead to the release of tumor necrosis factor-α (TNFα) from satellite cells. TNFα in turn potentiates the P2X3 receptor-mediated responses and increases the excitability of DRG neurons. This study provides strong evidence that somata of DRG neurons actively release transmitters and play a crucial role in bidirectional communication between neurons and surrounding satellite glial cells. These results also suggest that, contrary to the conventional view, neuronal somata have a significant role in cell–cell signaling.

neuron–glia communication | somatic release | P2X3 | P2X7 | tumor necrosis factor α

Neurons use transmitters released from vesicles at presynaptic terminals to communicate with other cells (1). Recent reports suggest that transmitter release also takes place in extrasynaptic domains (ectopic release) (2). It has been assumed for a long time that the cell body (i.e., soma) of a neuron does not release transmitters in response to electrical stimulation. This assumption has been challenged by our and others' observations that neuronal somatic release indeed occurs (3–10). Using carbon fibers, several groups have shown that somatic release of catecholamine occurs through vesicular mechanisms (3, 5–7). Exocytosis in response to membrane depolarization has also been reported in the somata of dorsal root ganglion (DRG) neurons (4), a group of neurons responsible for transmitting touch, temperature and pain information from the periphery to the spinal cord (11). In most cases, soma release is triggered and enhanced by voltage-dependent Ca^{2+} channels (4–7, 10). Despite these studies, it is not known whether vesicular release of fast-acting transmitters, e.g., ATP or glutamate, occurs in the somata. The function of somatic release is poorly understood.

ATP has been shown to be released from nerve terminals and axons of DRG neurons (12, 13), and is involved in synaptic transmission at afferent-dorsal horn synapses (14) and neuron–glia signaling (15). Because ATP-activated P2X receptors become greatly sensitized after injury (16–19), ATP is a transmitter especially important for signaling injurious nociceptive information. We found that sniffer patches excised from cells over-expressed with a specific receptor can provide us with sufficient sensitivity and temporal resolution to monitor the transmitter release dynamically from the soma of a neuron. Using this technique, we probed the release of ATP from the somata of DRG neurons. Here, we show that electric stimulation elicits robust vesicular release of ATP from neuronal somata and thus triggers bidirectional communication between neurons and satellite cells.

Results

We asked first whether vesicular release of ATP occurs in the somata of DRG neurons. P2X2-EGFP receptors were overexpressed in HEK cells and used as the biosensor (i.e., sniffer patch method) (20). P2X2 receptors were chosen because they were easily expressed at a high level (≈200 pA/pF) in HEK cells and the receptor-mediated currents hardly inactivated (21). To mimic physiological conditions, all release experiments were performed at 35°C. An outside-out membrane patch was pulled from a P2X2-expressing HEK293 cell with a patch electrode and placed against the somatic membrane of a DRG neuron (Fig. 1*A*). When the DRG neuron was stimulated with a whole-cell patch electrode to evoke action potentials, miniature excitatory synaptic current (mEPSC)-like inward current spikes were detected by the sniffer pipette (Fig. 1*A*). As a negative control, sniffer patches excised from nontransfected HEK cells could not detect any activity. We showed that the current activity was mediated by P2X2 receptors, because the P2X antagonist PPADS (pyridoxal-phosphate-6-azophenyl-2′-4′-disulfonic acid) (30 μM) reversibly blocked the responses (Fig. 1 *Bi* and *C*). Apyrase (30 units), which hydrolyzes extracellular ATP, abolished the current responses (Fig. 1 *Bii* and *C*), suggesting that ATP is indeed released from the somata of DRG neurons. Because current events were dramatically reduced in an extracellular solution containing the Ca^{2+} chelator BAPTA (1,2-bis(2-aminophenoxy)ethane-N,N,N′,N′-tetraacetate) and 0 Ca^{2+} (Fig. 1 *Biii* and *C*), external Ca^{2+} entry is required for somatic ATP release.

The current responses were further characterized by analyzing their amplitude distribution. The current events were kinetically homogenous because the rise time and half-width distribution of release events could be fit well with a single Gaussian [supporting information (SI) Fig. 5]. The amplitude of events could be fit with multiple Gaussians of equally spaced peaks (Fig. 1*Di*), suggesting the quantal nature of the ATP release (quantal size = 3.6 ± 0.3 pA, $n = 4$). To determine whether large release events were derived from recruitment of larger vesicles, the distribution of cubed root

Author contributions: X.Z. and L.-Y.M.H. designed research; X.Z., Y.C., C.W., and L.-Y.M.H. performed research; X.Z., Y.C., C.W., and L.-Y.M.H. analyzed data; and X.Z. and L.-Y.M.H. wrote the paper.

The authors declare no conflict of interest.

This article is a PNAS Direct Submission.

Abbreviations: DRG, dorsal root ganglion; mEPSC, miniature excitatory synaptic current; PPADS, pyridoxal-phosphate-6-azophenyl-2′-4′-disulfonic acid; BAPTA, 1,2-bis(2-aminophenoxy)ethane-N,N,N′,N′-tetraacetate; DAB, diaminobenzidine; BBG, brilliant blue G; oxATP, oxidized ATP; FM, *N*-(3-triethylammonium propyl)-4-[4-(diethylamino)styryl] pyridinium dibromide.

*To whom correspondence should be addressed. E-mail: lmhuang@utmb.edu.

This article contains supporting information online at www.pnas.org/cgi/content/full/0611048104/DC1.

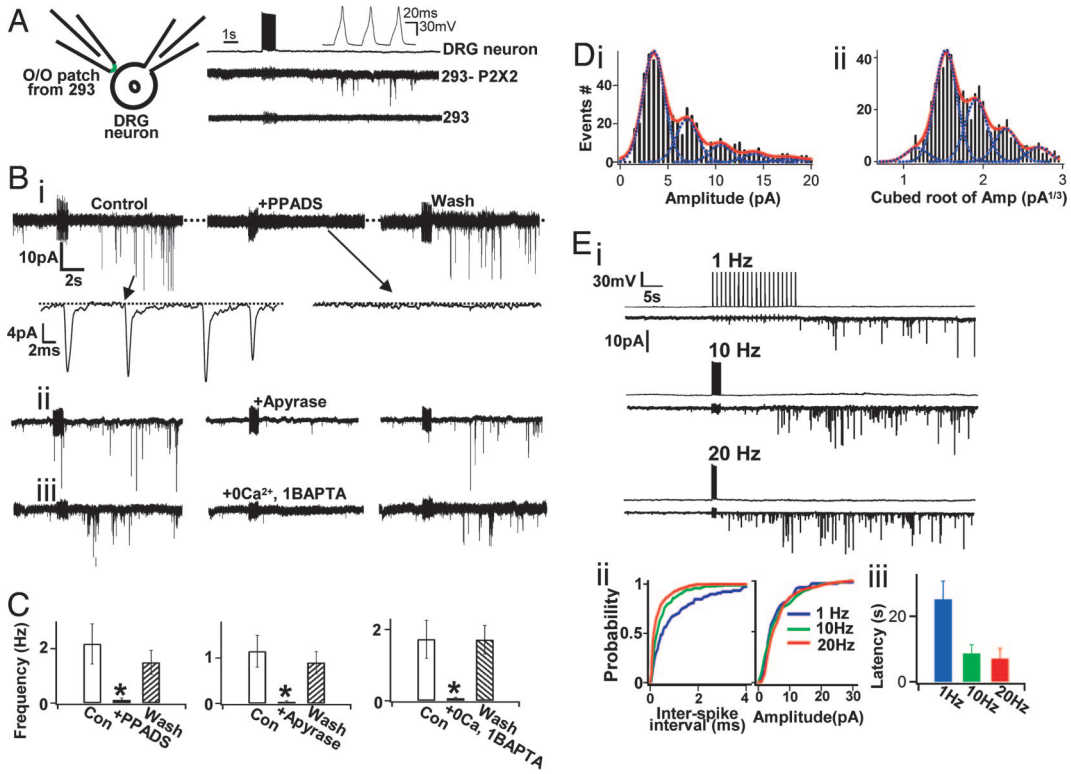

Fig. 1. ATP is released from the somata of cultured DRG neurons. (*A Left*) A schematic diagram of the setup used to study somatic ATP release through a sniffer patch pipette. (*A Right*) Examples of action potentials evoked by a 1-s, 20-Hz current stimulus train in a DRG neuron under current clamp conditions. The electrical stimulation evoked mEPSC-like spikes in a sniffer patch expressing P2X2-EGFP receptors and held at −80 mV. The same stimulus did not evoke any activity in another outside-out (O/O) patch excised from a nontransfected HEK cell. All experiments were done at 35°C. (*B*) Detected ATP release. After stimulation of a DRG neuron, mEPSC-like current responses were detected by a sniffer after a short delay. The activity usually dissipated in 2–5 min. Spikes with amplitudes larger than 2 times root-mean-square of the noise level were counted as release events. The arrow indicates release events shown on an expanded scale. The dotted line indicates the baseline. The same stimuli could not evoke any current responses when PPADS (30 μM), a P2X antagonist (*Bi*), or apyrase (30 units), an enzyme hydrolyzing ATP (*Bii*), was added to the bath solution. (*Biii*) The activity in a sniffer was abolished when the external solution was replaced by a solution containing 0 Ca^{2+} and 1 mM BAPTA. Data in *Bi* to *Biii* were obtained from three different sniffer patches. (*C Left*) Average block of current activity by PPADS. Control, 2.18 ± 0.74 Hz; PPADS, 0.12 ± 0.07 Hz; Wash, 1.50 ± 0.44 Hz ($n = 7$) (*, $P < 0.05$). (*C Center*) Average block of current activity by apyrase. Control, 1.15 ± 0.35 Hz; Apyrase, 0.04 ± 0.02 Hz; Wash, 0.90 ± 0.24 Hz ($n = 4$). (*C Right*) Average block of current activity by BAPTA. Control, 1.73 ± 0.54 Hz; BAPTA, 0.08 ± 0.03 Hz; Wash, 1.71 ± 0.40 Hz ($n = 5$). (*D*) Quantal nature of ATP release. (*Di*) Amplitude distribution of ATP release events could be fitted with multiple Gaussians of equally spaced peaks. In the data shown, the distribution was fit with five Gaussians with peaks separated by 3.5 pA. Mean quantum size = 3.6 ± 0.3 pA ($n = 4$). (*Dii*) After the cubed root transformation, the amplitude histogram remained multimodal. (*E*) Dependence of ATP release on stimulus frequency. (*Ei*) An example of release events recorded when twenty action potentials were evoked in DRG neurons at 1, 10, and 20 Hz. With increasing stimulus frequency, the events occurred more frequently. (*Eii*) With increasing stimulus frequencies, inter-spike intervals were shortened [Kolmogorov–Smirnov (KS) test, $P < 0.0001$], whereas the amplitude distribution did not change. (*Eiii*) The latency between the onset of the stimulus train to the first sniffer event decreased with increasing stimulus frequency (1 Hz, 25.2 ± 5.6 s; 10 Hz, 8.7 ± 2.7 s; 20 Hz, 7.1 ± 3.1 s, $n = 6$).

of peak amplitude of release events was analyzed. Cubed root transformation did not reveal any new bimodal Gaussian distribution, nor did it collapse the multipeak Gaussian distribution (Fig. 1*Dii*). Thus, ATP seems to be released synchronously from multiple vesicles rather than from different sized vesicles. The dependence of ATP release on stimulating frequency of neurons was also studied (Fig. 1*Ei*). Current activity at the sniffer was recorded when DRG neurons were stimulated by 20 action potentials delivered at 1, 10, or 20 Hz. To minimize vesicle depletion, different stimulus trains were given in a random order with a 7- to 8-min wait between the trains. With increasing frequency of stimulation, current events occurred at a higher rate and the interspike intervals were shortened whereas the amplitudes of the events remained unchanged (Fig. 1*Eii*). If the probability of somatic ATP release depends on the rate of $[Ca^{2+}]_i$ increase, the latency between the onset of the stimulation train to the first current spike should depend on stimulus frequency. We found that the latency indeed became progressively shorter as the frequency increased from 1 Hz to 20 Hz (Fig. 1*Eiii*).

We also examined exocytosis and endocytosis of vesicles in the somata of DRG neurons using FM1–43 (FM), a styryl dye that becomes fluorescent when it is partitioned in the membrane (22). An electrical stimulus (i.e., 20 Hz, 30 s) similar to that used to elicit ATP release was used to induce exocytosis. We found that vesicles in neuronal somata underwent robust exocytosis and were then retrieved by subsequent endocytosis (SI Fig. 6 *A* and *B*). Local vesicle recycling was not evident. Similar to the observation in sniffer patch experiments (Fig. 1), the total fluorescence increase depended on the stimulus frequency and external Ca^{2+} concentration (SI Fig. 6 *C* and *D*). The size and distribution of vesicles involved in the exo- and endocytosis were studied by using the photoconversion technique (23). Isolated DRG neurons were fixed within 10 s of neuronal stimulation and incubated in a diaminobenzidine (DAB) solution. The DAB in the FM1–43-containing vesicles was then photoconverted into an electron-dense reaction product and appeared darker than nonphotoconverted vesicles (Fig. 2*Ai* and SI Fig. 7). Under our experimental conditions, most photoconverted vesicles were scattered near the membrane. Rarely

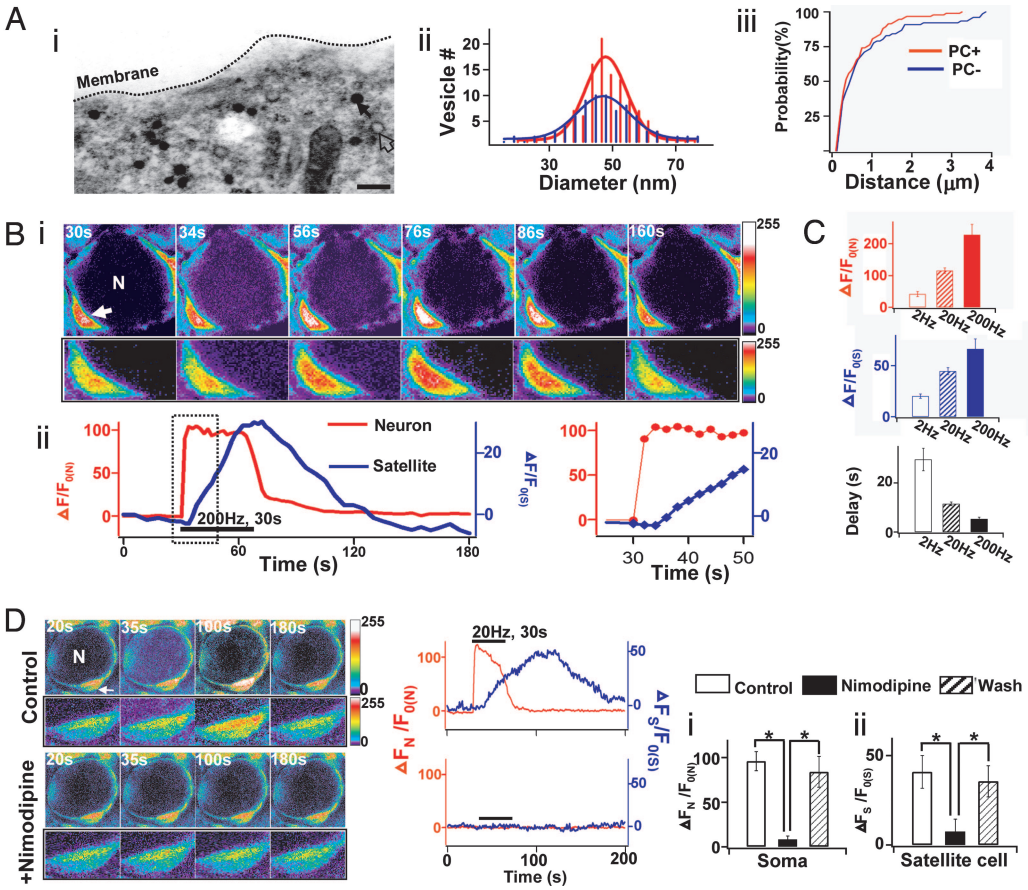

Fig. 2. Neuronal soma–satellite glial cell communication. (*A*) Small clear vesicles are involved in the release. (*Ai*) After FM1–43 application and electrical field stimulation to cultured DRG neurons at 20 Hz for 1 min, cells were fixed immediately, treated with DAB and viewed under an electron microscope. A clear (empty arrow) and a photoconverted vesicle (dark arrow) are indicated. (Scale bar: 100 nm.) (*Aii*) The size distribution of photoconverted (PC+) vesicles (red) was fit by a Gaussian with a mean diameter of 47.8 ± 6.5 (116 vesicles) (data were pooled from three experiments). The mean diameter of nonphotoconverted (PC−) vesicles (Blue) was 46.9 ± 8.3 (85 vesicles pools from three experiments), $P > 0.05$. (SI Fig. 7 for analysis). (*Aiii*) Cumulative histograms of the perpendicular distance of vesicles from the plasma membrane. Photoconverted vesicles were located closer to the plasma membrane than nonphotoconverted vesicles (KS test, $P = 0.0006$). (*B*) Nerve stimulation changes $[Ca^{2+}]_i$ responses in neurons and satellite cells in DRG ganglia. (*Bi*) Pseudocolor images of the fluorescence change in a neuron (N) and a satellite cell (arrow). The number at the upper left corner in each frame indicates the time at which the image was taken. Color-coded intensity calibration bar is shown on the right. Enlarged views of the satellite cell are shown directly below. Note a different color-coded calibration was used to highlight the fluorescence change in the satellite cell. Temperature = 35°C. Neuron diameter = 19.3 μm. (Time-lapse images are shown in SI Movie 2) (*Bii*) Time courses of relative fluorescence changes, i.e., $[(F - F_0)/F_0] = \Delta F/F_0$, in the neuron (red) ($\Delta F/F_{0(N)}$) and in the satellite cell (blue) ($\Delta F/F_{0(S)}$). F_0 is the basal fluorescence in either the neuron or the satellite cell before nerve stimulation. The horizontal line indicates the period of nerve stimulation. Responses in the dotted box are shown on an expanded scale to the right. Nerve stimulation (200 Hz, 30 s) evoked $[Ca^{2+}]_i$ increase in the neuron first and then in the satellite cell with a delay of 4.0 s. Compared with the $[Ca^{2+}]_i$ increase in the neuron, the $[Ca^{2+}]_i$ signal in the satellite cell had a later onset and a slower recovery. (*C*) Soma–satellite cell interactions depend on the frequency of nerve stimulation in the ganglia. With increasing stimulus frequency, the peak $[Ca^{2+}]_i$ in both neurons and satellite cells increased (neuron: 2 Hz, 42 ± 8%, $n = 4$; 20 Hz, 116 ± 9%, $n = 6$; 200 Hz, 228 ± 33%, $n = 6$; satellite cell: 2 Hz, 20 ± 2%, $n = 4$; 20 Hz, 45 ± 3%, $n = 6$, 200 Hz: 66 ± 10%, $n = 6$, $P < 0.05$). The delay between neurons and satellite cells also became shorter (2 Hz, 29.5 ± 4.6 s, $n = 4$; 20 Hz, 11.5 ± 0.8 s, $n = 6$; 200 Hz, 5.3 ± 0.8 s, $n = 6$, $P < 0.05$). (*D*) L-type voltage-dependent Ca^{2+} channels mediate the neuron-satellite cell interaction. The fluorescence increase evoked by nerve stimulation in both the neuron (N) and the satellite cell (arrow) was completely blocked by nimodipine (2 μM). Neuron diameter = 20.5 μm. (*Di*) In the neuronal somata, the change in $\Delta F/F_{0(N)}$ was 96.05 ± 10.78% in control, reduced to 8.40 ± 3.84% in nimodipine and returned to 84.09 ± 17.34% after wash ($n = 5$). (*Dii*) In satellite cells, $\Delta F_S/F_{0(S)}$ was 40.90 ± 9.14%, reduced to 7.57 ± 7.01% in nimodipine and returned to 35.70 ± 8.71% after wash ($n = 5$) (*, $P < 0.05$).

did they remain dock to the membrane surface. We have not seen vesicles aggregate at particular sites as those in presynaptic terminals. Photoconverted vesicles had a mean diameter of 47.8 ± 6.5 nm, similar to that of nonphotoconverted vesicles (46.9 ± 8.3 nm) (Fig. 2*Aii*). Measuring the perpendicular distance between vesicles and the membrane, we found that photoconverted vesicles were located closer to the plasma membrane than that of nonphotoconverted vesicles (Fig. 2*Aiii*). With our stimulus protocol, photoconverted large dense core vesicles were not seen. Only when neurons underwent strong and prolonged (>10 min) stimulation did we find large (diameter >100 nm) DAB-stained vesicles (data not shown).

The function of somatic release of DRG neurons was studied next. Although neuronal cell bodies are densely packed in the ganglion, they do not seem to make direct contact with each other (24). No morphologically defined synapses between cell bodies have been found. Instead, each soma is enwrapped by a layer of satellite glial cells. A likely function of somatic ATP release is neuron-satellite cell communication. To determine whether this communication indeed occurs, an L4 or L5 DRG with attached sciatic nerves was isolated from the rat, loaded with the fluorescence Ca^{2+} dye, Fluo-4 AM, and imaged under a confocal microscope. The basal fluorescence intensity (F_0) measured before the nerve stimulation, was five to eight times lower in neurons than F_0 in satellite cells (SI Movie 1). In response to nerve stimulation, neurons always fluoresced first. The surrounding satellite cells then lit up after a delay (Fig. 2*Bi*). Analyzing the time course of $[Ca^{2+}]_i$ increase, we

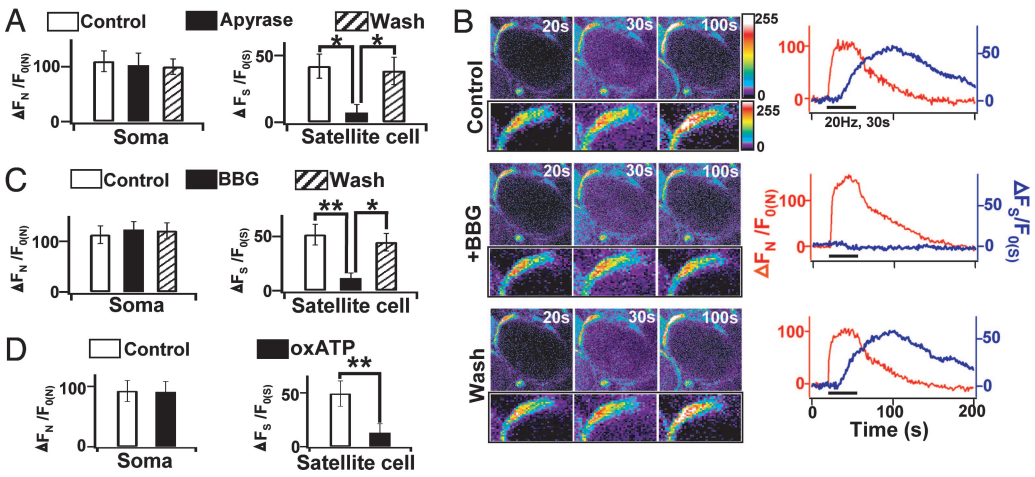

Fig. 3. P2X7 receptors are involved in the neuronal soma-satellite cell interaction. (*A*) Apyrase blocks $[Ca^{2+}]_i$ in satellite cells. Apyrase (30 U) had no effect on the $\Delta F_N/F_{0(N)}$ increase in the somata (Control, 110.13 ± 19.18%; apyrase, 102.89 ± 22.10%; Wash, 100.28 ± 14.06%; $P > 0.05$, $n = 4$), but blocked the $\Delta F_S/F_{0(S)}$ increase in satellite cells (Control, 42.06 ± 9.07%; apyrase, 7.26 ± 6.03%; Wash, 38.65 ± 10.27%; $n = 9$). (**, $P < 0.01$; *, $P < 0.05$). (*B*) An example of the BBG effect on the $[Ca^{2+}]_i$ increase in a neuron and a satellite cell in the ganglion. BBG (1 μM) inhibited the $[Ca^{2+}]_i$ increase in the satellite cell but had no effect on $[Ca^{2+}]_i$ increase in the neuron. Neuron diameter = 30.2 μm. (See SI Movies 3 and 4 for time-lapse images). (*C*) Average BBG blocking action. BBG did not change $\Delta F_N/F_{0(N)}$ in somata (Control, 113.13 ± 17.42%; BBG, 123.29 ± 15.70%; Wash, 120.87 ± 15.77%; $n = 7$, $P > 0.05$). However, it blocked the $\Delta F_S/F_{0(S)}$ increase in satellite cells (Control, 51.79 ± 9.54%; BBG, 11.61 ± 4.63%; wash, 44.94 ± 8.07%, $n = 15$). (*D*) The effect of the irreversible P2X7 blocker, oxATP. OxATP had no effect on the $\Delta F_N/F_{0(N)}$ increase in somata (Control, 92.56 ± 17.40%; oxATP: 91.06 ± 17.09%; $P > 0.05$, $n = 4$), but inhibited the $\Delta F_S/F_{0(S)}$ increase in satellite cells (Control, 49.30 ± 11.79%; oxATP, 12.90 ± 8.49%; $P < 0.01$, $n = 9$).

found that the $[Ca^{2+}]_i$ in neurons increased sharply after nerve stimulation, reaching a peak level within 1–2 s and remained at the plateau level (Fig. 2*Bii*). When the nerve stimulation was terminated, the $[Ca^{2+}]_i$ in neurons dropped rather quickly and returned to the basal level 20–30 s later. The rate of $[Ca^{2+}]_i$ changes in satellite cells was much slower. $[Ca^{2+}]_i$ in satellite cells reached its peak 10–30 s later. The $[Ca^{2+}]_i$ often stayed at a plateau level or continued to rise even after the nerve stimulation and then slowly (60–80 s) returned to the baseline (Fig. 2*Bii*).

As the stimulus frequency was increased from 2 to 200 Hz, the change in peak $[Ca^{2+}]_i$ in both neurons and satellite cells increased and the delay between the neuronal and satellite Ca^{2+} signals became shorter (Fig. 2*C*). L-type Ca^{2+} channel blocker, nimodipine (2 μM), completely blocked the $[Ca^{2+}]_i$ increase in both neurons and satellite cells, suggesting that activation of L-type Ca^{2+} channels is essential for the communication between neuronal somata and satellite cells (Fig. 2*D*).

To identify the transmitter involved in the communication, apyrase was again tested. We found that apyrase blocked the Ca^{2+} responses in satellite cells but had no effect on the Ca^{2+} responses in neurons (Fig. 3*A*). Thus, ATP released from neurons is the major transmitter participating in neuron-satellite cell communication. To determine the type of P2X receptors involved in the communication, the effects of the reversible P2X7 receptor antagonist brilliant blue G (BBG) and the irreversible P2X7 antagonist oxidized ATP (oxATP) were examined. Both BBG and oxATP blocked $[Ca^{2+}]_i$ increase only in satellite cells, but not in neurons (Fig. 3 *B–D*), suggesting that ATP released from neurons activates P2X7 receptors in satellite cells. In addition, BBG was found to block the KCl-induced $[Ca^{2+}]_i$ increase in satellite cells without affecting the $[Ca^{2+}]_i$ changes in neurons (SI Fig. 8), further confirming that ATP release is required for the correlated $[Ca^{2+}]_i$ change between neurons and satellite cells in response to nerve stimulation

To determine the consequence of P2X7 receptor activation in satellite cells, we studied the release of TNFα, a cytokine that is up-regulated after inflammation and nerve injury (25, 26) and exerts pronociceptive actions on sensory neurons (27–29). TNFα release before stimulation was below the detection level (< 6.25 pg/mg) (Fig. 4*A*). After tetanic trains of stimulation, TNFα release increased significantly (36.6 ± 6.1 pg/mg, $n = 3$). When DRGs were preincubated with oxATP (100 μM), the TNFα release was reduced by 77% (to 8.5 ± 1.2 pg/mg) (Fig. 4*A*). P2X7 receptor activation in satellite cells is likely the mechanism mediating the oxATP-dependent TNFα release in the ganglion. We then studied the actions of TNFα on neuronal activity in isolated DRG neurons. Low levels (0.5 ng/ml) of TNFα enhanced P2X3-receptor mediated currents in neurons (Fig. 4*B*). TNFα, at 12.5 ng/ml, was found to increase the excitability of neurons (Fig. 4*C*). These results suggest that under tetanic nerve stimulation, a condition mimicking cellular responses to inflammation and nerve injury, P2X7 receptor-dependent release of TNFα affects the activity of neurons.

Discussion

The overexpression of P2X2 receptors in sniffer patches allows us to unequivocally identify ATP released from the somata of DRG neurons (Fig. 1*Bi*). This conclusion is further confirmed by the result that release events disappeared in the presence of apyrase (Fig. 1 *Bii* and *C*). ATP release is vesicular because (*i*) sniffer patches detected discrete mEPSC-like release events at the somata of DRG neurons after action potential stimulation (Fig. 1*B*) and (*ii*) the amplitude of release events exhibits quantal Gaussian distribution (Fig. 1*Di*). Because the amplitude histogram of kinetically homogenous release events remains multimodal after cubed root transformation (Fig. 1*Dii*), multivesicular release of ATP from somata of DRG neurons is likely to occur. ATP has been shown to be stored and released from distinct pools of vesicles in hippocampal synapses (30), but is costored and coreleased in chromaffin cells (31) and hypothalamic neurons (32). It would be of interest to determine whether other transmitters, e.g., glutamate and 5HT, can be coreleased with ATP from neuronal somata. Our FM1–43 experiments confirmed that DRG somata undergo exocytosis and endocytosis in response to electrical stimulation (SI Fig. 6). Photoconversion experiments suggest that small clear vesicles participate in the exocytosis. Because FM1–43 experiments do not reveal the content of exocytic vesicles, one could not be sure that ATP was present in the observed small photoconverted vesicles. We suggest that small vesicles are likely to be involved in ATP release because

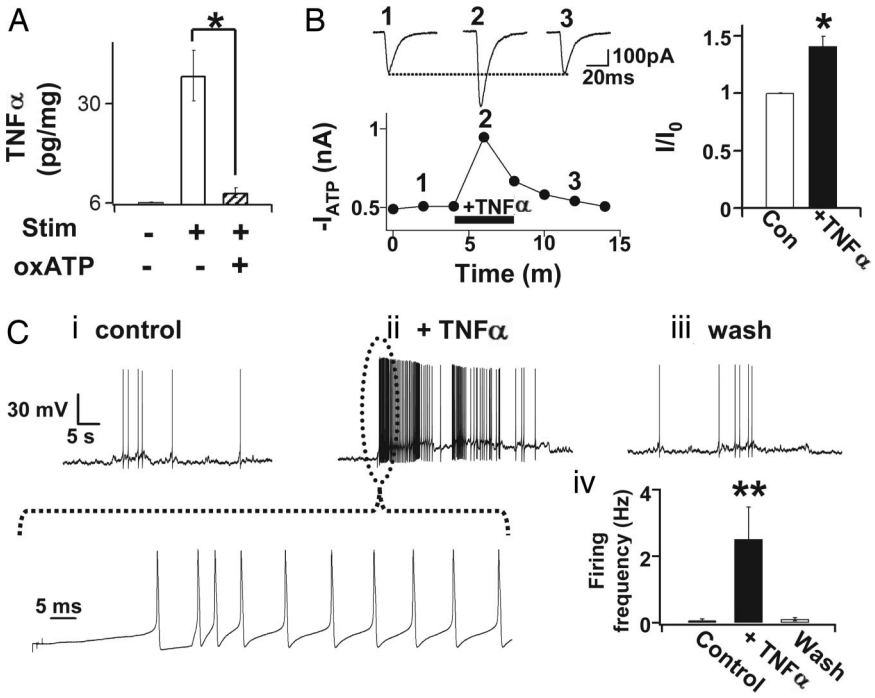

Fig. 4. TNFα released by P2X7 receptor activation changes neuronal activity. (*A*) Nerve stimulation increases the release of TNFα from ganglia. Prolonged tetanic stimulation induced TNFα release (36.6 ± 6.1 pg/mg, $n = 3$). Preincubation of ganglia with oxATP (100 μM) reduced the release of TNFα by 77% (to 8.5 ± 1.2 pg/mg, $n = 3$) (*, $P < 0.05$). Experiments were done at 35°C. (*B*) TNFα increases P2X3-mediated currents in cultured DRG neurons. TNFα (0.5 ng/ml) transiently increased P2X3 receptor-mediated ATP currents by 40.6 ± 8.5% ($n = 5$); *, $P < 0.05$. Holding potential = −60 mV, temperature = ≈23°C (*C*) TNFα also increases the firing in cultured DRG neurons. (*Ci*) Under current clamp conditions, this cell exhibited spontaneously firing. (*Cii*) in the presence of TNFα (12.5 ng/ml), the spontaneous firing in the DRG neuron was greatly potentiated. (*Ciii*) Wash. (*Civ*) TNFα potentiated the average firing frequency of DRG neurons (Control, 0.07 ± 0.04 Hz; TNFα, 2.51 ± 0.97 Hz, $P < 0.05$; Wash, 0.11 ± 0.05 Hz, $n = 5$). Temperature = ≈23°C.

P2X2 receptor-mediated mEPSC responses could be observed under similar electrical stimulus (Fig. 1).

It is interesting to note that neuronal somatic release is distinctly different from synaptic release, but closely resembles the regulated exocytosis in endocrine cells. For example, in the soma, there is no obvious structural correlate of the presynaptic thickening (i.e., active zone) where numerous small clear vesicles aggregate. Instead, vesicles in the neuronal soma are randomly distributed, many of them are located away from the membrane (Fig. 2*A*) (7), a distribution similar to those found in endocrine or PC12 cells (33). Another important difference between somatic release and synaptic release is the types of voltage-dependent Ca^{2+} channels involved in the release. We (Fig. 2*D*) and others (7, 10) have found that L-type Ca^{2+} channels, which are known to be loosely associated with release machinery (34, 35), mediate somatic exocytosis. In contrast, N- and P/Q types Ca^{2+} channels, which are closely associated with fusion machinery, are involved in the exocytosis at synaptic terminals (34, 36). These observations also are consistent with our conclusion that the intracellular Ca^{2+} levels required for somatic release is lower than those required for the release from most nerve terminals (4, 36).

One of the most interesting findings of our study is that somatic release of ATP in response to nerve stimulation plays a pivotal role in neuron-satellite glial cell communication in DRGs. These results revise our view that the soma of a neuron is primarily responsible for synthesis of molecules and has only a minor role in communication with other cells. Our study showed that the P2X7 blockers, BBG and oxATP completely block nerve-stimulated and KCl-induced $[Ca^{2+}]_i$ increase in satellite cells without affecting $[Ca^{2+}]_i$ transients in neurons (Fig. 3 and SI Fig. 8). These results, together with the finding that P2X7 receptors are expressed only in satellite cells in DRGs (37, 38), suggest that somatic ATP released from DRG neurons directly affects the activity of satellite cells by activation of P2X7 receptors. The slow $[Ca^{2+}]_i$ transients observed in satellite cells (Fig. 2*B*) is also consistent with the slow P2X7 receptor-mediated Ca^{2+} entry (39, 40). The involvement of P2X7 in the communication provides a mechanism by which neuronal somata convey information to satellite cells and receive feedback from them. Our results also suggest that neuronal somata could communicate with each other in the ganglia by propagating information through neuronal-glial chains.

The role of P2X7 in processing nociceptive signals has only been recently recognized. Inhibition of P2X7 receptors improves functional recovery in rats with spinal cord injury (41) and P2X7 knockout mice do not develop neuropathic pain after nerve ligation (42). The channel properties of P2X7 receptors are unusual. They require high concentration of ATP for their activation (21); the ion permeability of the P2X7 receptor channel depends on channel activity. Responding to prolonged or repeated stimulation, the channel becomes increasingly less selective, i.e., pore dilation (43, 44). These unique channel properties allow P2X7 receptors to respond dynamically to different pain states as ATP release from activated neurona or glial cells increases under various pathological conditions (17, 45)

In addition, P2X7 receptors have been found to be closely associated with cytokine functions. Activation of P2X7 receptors can lead to maturation and release of cytokines from glial cells (46). We showed that TNFα release by glial cells in ganglia is P2X7 receptor-mediated (Fig. 4). Exogenously applied TNFα can increase the firing of peripheral terminals (27), depolarize DRG neurons in ganglia (29) and increase the excitability of dissociated DRG neurons (Fig. 4). The mechanisms of TNFα action include reducing voltage-dependent K^+ currents, enhancing tetrodotoxin Na^+ channels (47), increasing capsaicin responses (28) and potentiating P2X3-receptor mediated currents (Fig. 4). It has yet to demonstrate that TNFα produced by activation of satellite cells

alters the excitability of neuronal somata *in vivo*. The release of TNFα occurring after tetanic nerve stimulation or injury would then affect neuronal activity and establish a positive feedback loop between neurons and satellite cells, thus contributing to exaggerated responses under pathological conditions. Our results emphasize the importance of soma–glia cell communication. There is evidence that neuronal somata also communicate directly with each other through cross-excitation (48), through purinergic synapses in cultures (49) or through noradrenergic synapses after peripheral nerve injury (50). It would be important to determine the relationship between soma–glia and soma–soma interactions and how it contributes to the complex communication among DRG cells. Harnessing such interactions in DRGs could be a new strategy for the treatment of chronic pain.

Materials and Methods

Electrophysiology. The sniffer patch method (20) was used to detect somatic ATP release. HEK293 cells were transfected with P2X2 plasmid (kindly provided by A. Surprenant, University of Sheffield, Sheffield, U.K.) tagged with enhanced GFP using FuGENE 6 (Roche, Indianapolis, IN). On the day of experiments, acutely dissociated DRG neurons were prepared from L4 or L5 DRGs of 21- to 28-day-old rats by using the method described in ref. 18. Within 6 h, release experiments were performed on small and medium (diameter $\leq$35 μm) DRG neurons at 35°C. To study the effects of TNFα on ATP currents, whole cell ATP currents were recorded from acutely dissociated DRG neurons at room temperature ($\approx$23°C). The use and care of experimental animals were according to institutional guidelines of the University of Texas Medical Branch, Galveston, TX.

FM1–43 Uptake and Photoconversion. FM1–43 uptake experiments were done on isolated DRG neurons at 35°C. After perfusion of FM1–43 (2 μM), DRG neurons were electrically stimulated with field stimulation. For photoconversion experiments, after FM1–43 application and electrical stimulation, neurons were fixed immediately with a glutaraldehyde (2%)-containing phosphate buffer saline (PBS) (100 mM) for 20 min and washed thoroughly to reduce autofluorescence. Afterward, neurons were incubated in DAB (1.5 mg/ml in PB) solution for 20 min and then illuminated with a 488-nm Argon laser light for 10–20 min while an ice-cold DAB solution was continuously refreshed. After photoconversion, neurons were washed in an ice-cold PB, and processed for electron microscopy (EM).

Calcium Imaging. Calcium imaging was done on whole ganglia. L4 or L5 DRGs were excised with the sciatic nerve attached. After the removal of meningeal layers, ganglia were recovered in an artificial cerebrospinal fluid (ACSF) solution for 1 h at 23°C. The ganglia were then incubated in a Fluo-4 AM (0.92 mM)-containing ACSF for 1 h. After wash, a ganglion was then placed under a Nikon upright confocal microscope (Melville, NY). Bipolar electrode was placed on the sciatic nerve to stimulate the axons of DRG neurons. Imaging analysis was done with the Metamorph software (Downingtown, PA).

Release of TNFα. A L4 or L5 DRG with the sciatic nerve attached was placed in a chamber containing 200 μl external solution. A bipolar electrode was placed on the sciatic nerve to apply tetanic stimulation (12.5-, 25-, and 50-Hz pulse sequence applied for 5 min each and the sequence was repeated four times) at 35°C. The solution was collected. Solution samples from four DRGs were pooled together and concentrated. The TNFα concentration was measured by using an ELISA kit (R & D Systems, Minneapolis, MN). The release values were normalized with the protein content in DRGs, which was determined afterward by a colorimetric assay by using bicinchoninic acid (BCA).

Statistical Analysis. Data are expressed as mean $\pm$ SEM. Tests for significance ($P < 0.05$) were made either with the Student's t test or with the analysis of variance (ANOVA), followed by Newman Keuls post hoc tests.

For detailed description of the methods, see *SI Materials and Methods*.

We thank Drs. W Betz, Y. Gu, H. Fishman, A. Ritchie, G. Swanson, and W. Willis for comments; and Dr. S. Carlton and Ms. Z. Ding for processing EM samples and photographs. This work was funded by National Institutes of Health Grants NS30045 and DE17813 (to L.-Y.M.H.).

1. Stevens CF (2003) *Neuron* 40:381–388.
2. Matsui K, Jahr CE (2006) *Curr Opin Neurobiol* 16:305–311.
3. Chen G, Gavin PF, Luo G, Ewing AG (1995) *J Neurosci* 15:7747–7755.
4. Huang LY, Neher E (1996) *Neuron* 17:135–145.
5. Jaffe EH, Marty A, Schulte A, Chow RH (1998) *J Neurosci* 18:3548–3553.
6. Bruns D, Riedel D, Klingauf J, Jahn R (2000) *Neuron* 28:205–220.
7. Puopolo M, Hochstetler SE, Gustincich S, Wightman RM, Raviola E (2001) *Neuron* 30:211–225.
8. Matsuka Y, Neubert JK, Maidment NT, Spigelman I (2001) *Brain Res* 915:248–255.
9. Zhang C, Zhou Z (2002) *Nat Neurosci* 5:425–430.
10. Trueta C, Mendez B, De-Miguel FF (2003) *J Physiol (London)* 547:405–416.
11. Willis WD, Coggeshall RE (2004) in *Sensory Mechanisms of the Spinal Cord* (Kluwer Academic/Plenum Publishers, New York), Vol 1, pp 91–101.
12. Soeda H, Tatsumi H, Katayama Y (1997) *Neuroscience* 77:1187–1199.
13. Stevens B, Fields RD (2000) *Science* 287:2267–2271.
14. Engelman HS, MacDermott AB (2004) *Nat Rev Neurosci* 5:135–145.
15. Fields RD, Burnstock G (2006) *Nat Rev Neurosci* 7:423–436.
16. Cook SP, Vulchanova L, Hargreaves KM, Elde R, McCleskey EW (1997) *Nature* 387:505–508.
17. Chen Y, Li GW, Wang C, Gu Y, Huang LY (2005) *Pain* 119:38–48.
18. Xu GY, Huang LY (2002) *J Neurosci* 22:93–102.
19. Hamilton SG, Wade A, McMahon SB (1999) *Br J Pharmacol* 126:326–332.
20. Allen TG (1997) *Trends Neurosci* 20:192–197.
21. North RA (2002) *Physiol Rev* 82:1013–1067.
22. Betz WJ, Mao F, Bewick GS (1992) *J Neurosci* 12:363–375.
23. Henkel AW, Lubke J, Betz WJ (1996) *Proc Natl Acad Sci USA* 93:1918–1923.
24. Hanani M (2005) *Brain Res Brain Res Rev* 48:457–476.
25. McMahon SB, Cafferty WB, Marchand F (2005) *Exp Neurol* 192:444–462.
26. Watkins LR, Milligan ED, Maier SF (2003) *Adv Exp Med Biol* 521:1–21.
27. Schafers M, Lee DH, Brors D, Yaksh TL, Sorkin LS (2003) *J Neurosci* 23:3028–3038.
28. Nicol GD, Lopshire JC, Pafford CM (1997) *J Neurosci* 17:975–982.
29. Liu B, Li H, Brull SJ, Zhang JM (2002) *J Neurophysiol* 88:1393–1399.
30. Pankratov Y, Lalo U, Verkhratsky A, North RA (2006) *Pflugers Arch* 452:589–597.
31. Hollins B, Ikeda SR (1997) *J Neurophysiol* 78:3069–3076.
32. Jo YH, Role LW (2002) *J Neurosci* 22:4794–4804.
33. Liu TT, Kishimoto T, Hatakeyama H, Nemoto T, Takahashi N, Kasai H (2005) *J Physiol (London)* 568:917–929.
34. Lara B, Gandia L, Martinez-Sierra R, Torres A, Garcia AG (1998) *Pflugers Arch* 435:472–478.
35. Neher E (1998) *Neuron* 20:389–399.
36. Augustine GJ, Santamaria F, Tanaka K (2003) *Neuron* 40:331–346.
37. Kobayashi K, Fukuoka T, Yamanaka H, Dai Y, Obata K, Tokunaga A, Noguchi K (2005) *J Comp Neurol* 481:377–390.
38. Zhang XF, Han P, Faltynek CR, Jarvis MF, Shieh CC (2005) *Brain Res* 1052:63–70.
39. Suadicani SO, Brosnan CF, Scemes E (2006) *J Neurosci* 26:1378–1385.
40. He ML, Zemkova H, Koshimizu TA, Tomic M, Stojilkovic SS (2003) *Am J Physiol Cell Physiol* 285:C467–79.
41. Wang X, Arcuino G, Takano T, Lin J, Peng WG, Wan P, Li P, Xu Q, Liu QS, Goldman SA, Nedergaard M (2004) *Nat Med* 10:821–827.
42. Chessell IP, Hatcher JP, Bountra C, Michel AD, Hughes JP, Green P, Egerton J, Murfin M, Richardson J, Peck WL, *et al.* (2005) *Pain* 114:386–396.
43. Khakh BS, Bao XR, Labarca C, Lester HA (1999) *Nat Neurosci* 2:322–330.
44. Virginio C, MacKenzie A, Rassendren FA, North RA, Surprenant A (1999) *Nat Neurosci* 2:315–321.
45. Franke H, Krugel U, Illes P (2006) *Pflugers Arch* 452:622–644.
46. Colomar A, Marty V, Medina C, Combe C, Parnet P, Amedee T (2003) *J Biol Chem* 278:30732–30740.
47. Jin X, Gereau RW t. (2006) *J Neurosci* 26:246–255.
48. Amir R, Devor M (1996) *J Neurosci* 16:4733–4741.
49. Zarei MM, Toro B, McCleskey EW (2004) *Neuroscience* 126:195–201.
50. McLachlan EM, Hu P (1998) *Neuroscience* 84:961–965.